Comparison of Extreme Coastal Flooding Events between Tropical and Midlatitude Weather Systems in the Delaware and Chesapeake Bays for 1980–2019

JOHN A. CALLAHAN, DANIEL J. LEATHERS, A, AND CHRISTINA L. CALLAHAN L.

^a Department of Geography and Spatial Sciences, University of Delaware, Newark, Delaware ^b Center for Environmental Monitoring and Analysis, University of Delaware, Newark, Delaware

(Manuscript received 19 April 2021, in final form 20 January 2022)

ABSTRACT: Coastal flooding is one of the most costly and deadly natural hazards facing the U.S. mid-Atlantic region today. Impacts in this heavily populated and economically significant region are caused by a combination of the location's exposure and natural forcing from storms and sea level rise. Tropical cyclones (TCs) and midlatitude (ML) weather systems each have caused extreme coastal flooding in the region. Skew surge was computed over each tidal cycle for the past 40 years (1980–2019) at several tide gauges in the Delaware and Chesapeake Bays to compare the meteorological component of surge for each weather type. Although TCs cause higher mean surges, ML weather systems can produce surges just as severe and occur much more frequently, peaking in the cold season (November–March). Of the top 10 largest surge events, TCs account for 30%–45% in the Delaware and upper Chesapeake Bays and 40%–45% in the lower Chesapeake Bay. This percentage drops to 10%–15% for larger numbers of events in all regions. Mean sea level pressure and 500-hPa geopotential height (GPH) fields of the top 10 surge events from ML weather systems show a low pressure center west-southwest of "Delmarva" and a semistationary high pressure center to the northeast prior to maximum surge, producing strong easterly winds. Low pressure centers intensify under upper-level divergence as they travel eastward, and the high pressure centers are near the GPH ridges. During lower-bay events, the low pressure centers develop farther south, intensifying over warmer coastal waters, with a south-shifted GPH pattern relative to upper-bay events.

SIGNIFICANCE STATEMENT: Severe coastal flooding is a year-round threat in the U.S. mid-Atlantic region, and impacts are projected to increase in magnitude and frequency. Research into the meteorological contribution to storm surge, separate from mean sea level and tidal phase, will increase the scientific understanding and monitoring of changing atmospheric conditions. Tropical cyclones and midlatitude weather systems both significantly impact the mid-Atlantic region during different times of year. However, climate change may alter the future behavior of these systems differently. Understanding the synoptic environment and quantifying the surge response and subbay geographic variability of each weather system in this region will aid in public awareness, near-term emergency preparation, and long-term planning for coastal storms.

KEYWORDS: Extratropical cyclones; Extreme events; Flood events; Storm surges; Tropical cyclones; Severe storms; North Atlantic Ocean

1. Introduction

Although coastal storms are well known as a multithreat hazard along the U.S. East Coast, bringing heavy precipitation, strong winds, large waves, and rip currents, it is coastal flooding that poses the greatest threat to human life and is often the source of much of the damage (Blake and Gibney 2011; Rappaport 2014; Rajan and Saud 2018; Weinkle et al. 2018). The mid-Atlantic region is especially prone to the severe impacts of coastal flooding as both economically critical human infrastructure and important natural ecosystems are found along its coasts (Sanchez et al. 2012; Haaf et al. 2017; Chesapeake Bay Program 2020). Under current climate change model projections, mean sea levels are expected to

© Supplemental information related to this paper is available at the Journals Online website: https://doi.org/10.1175/JAMC-D-21-0077.s1.

Corresponding author: John A. Callahan, john.callahan@udel.edu

increase globally and regionally at accelerated rates (Sweet et al. 2017b; Oppenheimer et al. 2019). Consequently, the mid-Atlantic region's high rates of sea level rise (SLR) (Sallenger et al. 2012; Boon et al. 2018; Piecuch et al. 2018) lead directly to increases in high-tide flood frequency (Moftakhari et al. 2015; Sweet et al. 2018; Sweet et al. 2020) and in the probability of storm-based major coastal flooding events (Lin et al. 2016; Dahl et al. 2017; Rahmstorf 2017; Garner et al. 2017; Muis et al. 2020; Taherkhani et al. 2020).

Extreme coastal flooding events can have profound negative effects as they usually include multiple hazards that compound the damage, leading to the net impact to be greater than the sum of its parts (Kopp et al. 2017; Moftakhari et al. 2015; Martzikos et al. 2021). Impacts and costs associated with coastal flooding are highly dependent upon natural and social vulnerability, the amount of exposure, and adaptation measures in place (Hallegatte et al. 2013; Hinkel et al. 2014). Varying adaptive capacity and sensitivity of coastal exposure of the wide range of land-use activities results in differing vulnerabilities across the mid-Atlantic (Domingues et al. 2020). Local states/municipalities in this region view coastal flooding

DOI: 10.1175/JAMC-D-21-0077.1

as one of the most severe and pervasive natural hazards and have been active in their applied research and planning (Callahan et al. 2017; Boesch et al. 2018; Dupigny-Giroux et al. 2018).

Meteorologically, the mid-Atlantic United States lies in a climatic transition zone between continental and marine climate types and is impacted by both tropical cyclones (TCs) and extratropical cyclones (ETCs) depending upon the time of year. TCs originate in the tropical and subtropical waters to the south-southeast from summer through midfall and have caused major coastal flooding to the region, most notably from Hurricanes Isabel (2003) and Sandy (2012). TCs typically bring stronger winds and higher surges but ETCs usually impact larger swaths of coastline (Pugh 2004; von Storch and Woth 2008). ETCs that impact the mid-Atlantic commonly originate to the west-northwest from late autumn through spring. Oftentimes, they are referred to as East Coast winter storms, particularly when associated with snow and ice, or as "nor'easters" when the ETC reaches the coast and intensifies over warmer waters (Hirsch et al. 2001; Zhang et al. 2000; Thompson et al. 2013; Leathers et al. 2011). Intensification and storm track of the ETCs are often dictated by the relative position of troughs and ridges in the westerly polar jet stream. ETC low pressure centers on the east side of upper-level troughs intensify under an area of upper-level divergence, and whose path along the coast is largely directed by upperlevel ridges and nearby high pressure systems present in the North Atlantic Ocean (Bernhardt and DeGaetano 2012; Leathers et al. 2011). ETCs are associated with the great majority of coastal flood events in the mid-Atlantic as compared with TCs, and those that intensify offshore (i.e., "nor'easters") often follow a more meridional path, causing them to travel slower and impact the region for longer periods of time (Dolan and Davis 1992; Zhang et al. 2000; Bernhardt and DeGaetano 2012; Colle et al. 2015; Booth et al. 2016; Catalano and Broccoli 2018). Some ETCs have caused damage on par with most TCs in the region (Delaware Emergency Management Agency 2018), such as the Ash Wednesday Storm of 1962, the pair of nor'easters in January-February 1998 (Ramsey et al. 1998), and the Mother's Day Storm of 2008.

Under current global warming scenarios, the frequency of major TCs, as well as their wind speed and pressure center, is expected to increase in the future (Knutson et al. 2019; Knutson et al. 2020), compounding the impacts from SLR alone. However, future projections of ETC development and storm-track position, and similarly for landfalling TCs, due to changing synoptic atmospheric patterns (i.e., "storminess") in the mid-Atlantic is inconclusive (Hall et al. 2016; Mawdsley and Haigh 2016; Michaelis et al. 2017; Dupigny-Giroux et al. 2018; Lin et al. 2019). It is critical that we understand the severity and geographic variability of storm surge to properly assess future risk, aid in preparedness, and ultimately reduce the severe impacts from coastal flooding (Council on Climate Preparedness and Resilience 2016).

Although several studies have investigated the difference between TC and ETC storm types on large coastal flooding events near New York (City), New York (NYC; DeGaetano

2008; Colle et al. 2010; Salmun et al. 2011; Lin et al. 2012; Talke et al. 2014; Garner et al. 2017), very few have focused within the mid-Atlantic. Booth et al. (2016) looked at all extreme storm surge events (greater than 1-yr return level) at a few selected tide gauges from Portland, Maine, to Duck, North Carolina. They found that for large coastal flood events covering a wider coastal area, tropical systems were the most likely cause, whereas for slightly less severe events and extent, the relative importance of TCs decreased and ETCs increased, with higher relative frequencies of TCs to the south. Wilkerson and Brubaker (2012) investigated the spatial variability of total water levels (rather than storm surge) in the central and lower Chesapeake Bay from both storm types. They found that central bay gauges spent more time over the typical tidal datum thresholds but had lower overall magnitudes, however, their study included only a small set of events (1998-2011) and did not analyze storm type events separately. Catalano and Broccoli (2018), focusing on the large-scale influences of ETC surge events at three locations covering a large swath of the U.S. East Coast (Boston, Massachusetts; the Battery, NYC; and Sewells Point, Virginia), noted a higher frequency and surge magnitude of TCs toward the south. Rashid et al. (2019), using a combined SLR + storm surge index based on tide gauge observations over the contiguous U.S. coastline, and Orton et al. (2016), using separate TC and ETC simulations at NYC, both concluded that characteristics of coastal flooding hazards driven by the two types of storms are different and suggested to consider them separately in flood risk assessments.

This paper will focus on the spatial variability of storm surge within the Delaware and Chesapeake Bays of the U.S. mid-Atlantic. Water levels in these bays have been well monitored for several decades by high-quality, tide gauge networks, well suited for climate studies (Holgate et al. 2013; Sweet et al. 2017a; NOAA 2020a,b). Extreme surge magnitude, distribution, month of occurrence, and relative frequency of events between TCs and midlatitude (ML) weather systems (encompassing ETCs, high pressure systems, and frontal systems) will be compared at numerous locations within the bays. This paper will also identify top ML surge events and investigate mean sea level pressure and 500-hPa geopotential height synoptic patterns.

To estimate the contribution of weather to coastal flood levels, as opposed to high tides and increases in mean water levels due to sea level rise, skew surge is used for this study. Skew surge is defined as the difference between the maximum total water level and the maximum predicted tide level over a tidal cycle, even if the observed and predicted tidal peaks are offset (i.e., skewed) from each other (Pugh and Woodworth 2014). The primary contributor to skew surge value is the conventional wind and pressure-driven storm surge, however, this measure also includes other contributors to the increased water levels, such as nearby river discharge from precipitation runoff and wave setup. Higher-frequency wave runup from high winds and breaking waves, a large factor in erosion and property damage, is also included in the computation of skew surge. However, this contribution to tide gauge measured still water levels is mitigated by the high-frequency attenuation of the harbors where the gauges are installed by design as well as the relatively shallower waters and broad shelf off the U.S. East Coast (Sweet et al. 2015). Overall, skew surge arguably better represents the sum of the meteorological components of coastal flooding above the astronomically forced tides and tide–surge interactions (Batstone et al. 2013; Mawdsley and Haigh 2016; Williams et al. 2016; Stephens et al. 2020). Additionally, tide gauges within the study area are grouped into subbay regions, each consisting of two or three adjacent tide gauges whose surge response and total water levels are more highly correlated to each other than to nonadjacent gauges. The list of top midlatitude surge events produced in this paper are based on ranking of average regional skew surge rather than at individual tide gauges.

Together with Callahan et al. (2021) and Callahan and Leathers (2021), these three papers provide an in-depth summary of the top surge events in the mid-Atlantic over the period 1980–2019. Severe coastal flooding is a year-round threat in the region and projected to increase in magnitude and frequency. Research into the meteorological component of coastal flooding and its spatial variability from multiple types of weather in the mid-Atlantic will not only improve scientific understanding, but it will also aid in public awareness, near-term emergency preparation, and long-term planning for coastal storms.

2. Study region

a. Delaware and Chesapeake Bays

The Delaware and Chesapeake Bays, connected via the Chesapeake and Delaware (C and D) Canal, are heavily tidally influenced, with freshwater inputs from the major river systems of the Delaware River, Susquehanna River, and Potomac River (Fig. 1). The Delaware Bay has a classical funnel shape, with pockets of deep scour in the wider lower bay, amplifying tidal range and storm surge in the northern regions (Wong and Münchow 1995; Lee et al. 2017; Ross et al. 2017). The Chesapeake Bay, by contrast is longer and shallower, with more dendritic tributary landscape and with the lowest tidal ranges toward the center (Zhong and Li 2006; Lee et al. 2017; Ross et al. 2017).

Although coastal storms threaten the region year-round, mean water levels follow a bimodal distribution with the maximum in midfall and secondary maximum in late spring, primarily caused by periodic fluctuations in atmospheric weather systems and coastal water steric effects (NOAA CO-OPS 2020a). Summer shows the lowest mean sea levels and usually the least number of coastal storms.

b. Tide gauge selection

Tide gauges selected for the current study were limited to NOAA operational tide gauges within or in the immediate vicinity of the Delaware and Chesapeake Bays. Requirements were that each gauge selected would have a nearly continuous record of hourly water levels over a common time period, a set of harmonic constituents identified for making tidal predictions, and tidal datum conversion factors to North

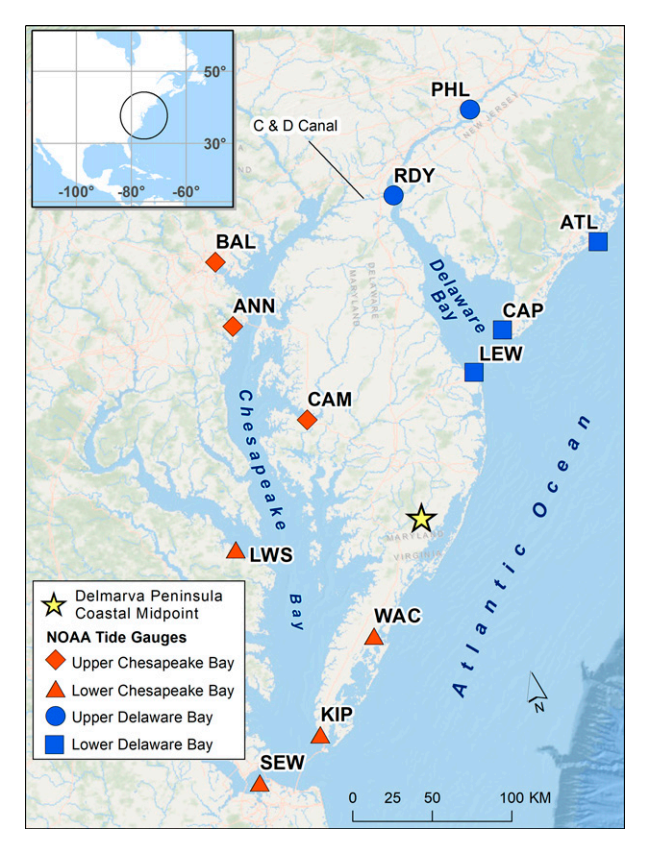


FIG. 1. Map of the Delaware and Chesapeake Bays with the 12 NOAA tide gauges used in the current study; the site labels are defined in section 2b. The figure is adapted from Callahan et al. (2021).

American Vertical Datum of 1988 (NAVD88). Based on the available data and findings from previous research in Callahan et al. (2021), 12 tide gauges and the time period 1980–2019 were selected. The gauges are spaced approximately evenly throughout the study area to address spatial variation in storm surge response. Five gauges are associated with the Delaware Bay, and seven are associated with the Chesapeake Bay (Table 1). All selected gauges are part of NOAA National Ocean Service National Water Level Observation Network (NWLON) and Physical Oceanographic Real-Time System (PORTS) networks.

In Callahan et al. (2021), cross-correlation and principal component analysis identified upper and lower-bay regions of tide gauges where surge and total water levels from TCs were highly correlated (Fig. 1). Regions are defined as the upper [Philadelphia (PHL) and Reedy Point (RDY)] and lower [Lewes (LEW), Cape May (CAP), and Atlantic City (ATL)] Delaware Bay and the upper [Baltimore (BAL), Annapolis (ANN), and Cambridge (CAM)] and lower [Sewells Point (SEW), Kiptopeke (KIP), and Wachapreague (WAC)] Chesapeake Bay. Note that the Lewisetta (LWS) gauge was not assigned to a region because the region with which it was most closely associated varied between the upper and lower Chesapeake Bay. Surges were correlated more strongly

TABLE 1. NOAA tide gauges with hourly water-level data covering 1980–2019 used in the current study. Percent of hourly data is based upon the maximum number of hours in 1980–2019. Here, ID indicates identification number.

Station	Code	NOAA ID	Bay	Hourly data
Philadelphia	PHL	8545240	Delaware	99.23%
Reedy Point	RDY	8551910	Delaware	95.61%
Lewes	LEW	8557380	Delaware	99.73%
Cape May	CAP	8536110	Delaware	98.35%
Atlantic City	ATL	8534720	Delaware	98.08%
Baltimore	BAL	8574680	Chesapeake	99.66%
Annapolis	ANN	8575512	Chesapeake	98.70%
Cambridge	CAM	8571892	Chesapeake	98.84%
Lewisetta	LWS	8635750	Chesapeake	98.72%
Kiptopeke	KIP	8632200	Chesapeake	99.78%
Sewells Point	SEW	8638610	Chesapeake	100.00%
Wachapreague	WAC	8631044	Chesapeake	89.30%

between the upper (or lower) regions across the bays than between the upper and lower region within a single bay.

3. Data and methods

 Water-level data processing and computation of skew surge levels

Hourly and high/low water-level data were obtained from the NOAA Center for Operational Oceanographic Products and Services (NOAA CO-OPS 2020b). Hourly data represent the observed water level on each hour (e.g., 2100 or 2200). High/low data represent the exact time and magnitude of each higher-high, high, low, and lower-low tidal peak. Data at each gauge were manually inspected for errors and inconsistencies. A few small data clusters (2-16 h) that existed within larger periods of missing data were removed (on seven occasions across all gauges) and small data gaps of 1-2 h (less than 10 across all gauges) were filled using linear interpolation. Table 1 lists the percent of hourly data available for analysis based upon the total number of hours in 1980-2019. All gauges had greater than 95% data availability except for the gauge at WAC (89%), due to a 2.5-yr period (November 2005-April 2008) when valid hourly and high/low data were unavailable.

Harmonic analysis was performed on the hourly water levels incorporating 37 tidal constituents defined by NOAA for their official tide predictions in this region (NOAA CO-OPS 2020c) and seven tidal constituents noted by Harris (1991) relevant for the U.S. East Coast to determine the predicted tide levels. Computations were carried out in 1-yr time intervals, or 3-yr intervals if greater than one continuous month of data was missing within a year. Annual computations minimize timing errors that can lead to the leakage of tidal energy into the nontidal residual (Merrifield et al. 2013), essentially remove the SLR trend, and minimize inherent constituent biases when computed over long time periods resulting from changing physiographic conditions in the bays (Ross et al. 2017) or changing seasonal weather patterns that largely affect the Sa (solar annual) and SSa (solar semiannual) constituents (Parker 2007). Skew surge was then computed as the

difference between the maximum observed total water level (TWL) from the high/low data and the maximum predicted tide level over each tidal cycle, even if the observed and predicted tidal peaks are offset (i.e., skewed) from each other (Pugh and Woodworth 2014). More details on the computation of skew surge can be found in Callahan et al. (2021).

Skew surge and TWL were then detrended about the 1980-2019 mean for each gauge. Total count was a maximum of 28231 tidal peaks over the full study time period less any missing data. All gauges showed statistically significant positive trends in TWL, whereas no gauges showed statistically significant trends in skew surge except for PHL, which showed a slight negative trend. To better compare magnitudes of storm-based flood levels at gauges with differing mean sea levels and tidal ranges, the skew surge time series was normalized (i.e., difference from the mean divided by standard deviation), resulting in a skew surge index (SSI) value for each tidal cycle. Tidal peaks during major coastal flooding events were also temporally declustered to focus on the event rather than on individual high-tide peaks. If multiple tidal peaks were above a selected water-level threshold and within 30 h of each other, they were treated as a single event and only the maximum value was chosen, ensuring at least two consecutive high tides between each event. Although ETCs can impact the region over multiple days, it is rare for a single system to cause multiple extreme water levels (or extreme storm surges) separated by two consecutive high tides that are both under an extreme threshold. A lower water-level threshold would have required a longer declustering time interval.

Extreme skew surge and TWL thresholds for this study are defined as the 6-month return level (RL). For TWL, this lies slightly above NWS minor coastal flood advisory levels by approximately 1-6 cm (Table S1 in the online supplemental material), defined by NWS as the level at which minimal or no property damage and possible threat to the public on average would occur in the nearby region, and below the NWS moderate coastal flood advisory level, defined as the level at which some inundation of structures and roads occurs near the stream and requires some evacuations of people and/or transfer of property to higher ground. All surge events in this study lie above the NWS minor coastal flood advisory level except at WAC where the 6-month return level is 1-2 cm below. Although this choice was arbitrary, the twice per year event was chosen to yield enough data points (approximately 80 events over 40 years) for statistical analysis and could potentially cause flood impacts. While water levels at the 6-month RL would not be typically considered extreme from an impact perspective, this is the low-end cutoff and all of our TWL and surge events are above this level. Return levels were estimated through traditional extreme value analysis on the detrended skew surge and TWL time series using the points-over-threshold (POT) sampling and fitting the exceedances to the generalized Pareto (GP) distribution. To perform extreme value analysis using the POT/GP approach, a threshold must first be chosen that would include enough upper tail exceedances to improve the robustness of the model but not too many exceedances such that the lower exceedances introduce bias from the parent distribution. This threshold was determined separately for each tide gauge following the sequential hypothesis testing method described in Callahan and Leathers (2021). Thresholds for skew surge were tested for percentages ranging from 90.0% to 99.5% in 0.5% increments, whereas for TWL, the range was 95.0%-99.5% as GP model fits using lower percentages (i.e., higher number of exceedances) failed to converge when estimating model parameters. Once a threshold was chosen, model parameters were estimated and the 6-month RL extracted at each gauge. The 6-month RLs were compared with the mean-higher high water (MHHW) and mean sea level (MSL) tidal data (or "datums") and their spatial variation. Since the tidal data were computed over the national tidal datum epoch (NTDE) of 1983-2001, these data were adjusted by adding the difference in mean TWL over the NTDE and the study period. The adjustments were small, ranging only from 0.03 to 0.05 m across the study area.

b. Storm-type identification

To identify whether a coastal flood event was caused by a TC or ML weather system, timing of the tidal peaks was compared with storm information in the International Best Track Archive for Climate Stewardship (IBTrACS) North Atlantic basin dataset, version 4 (Knapp et al. 2018). Storm systems listed in IBTrACS achieved a tropical cyclone classification (e.g., tropical depression, tropical storm, hurricane, subtropical depression, or subtropical storm) at some point in its lifetime and included all TCs that originated in the North Atlantic Ocean, Caribbean Sea, and Gulf of Mexico. Callahan et al. (2021) identified a subset of 144 TCs in IBTrACS over the period 1980-2019 with tracks that crossed within a 750-km-radius circular buffer around the "Delmarva" Peninsula (centered on 38.137778, -75.416944). Surface weather maps and storm reports were consulted for each of the 144 TCs to identify the presence of nontropical forcing (i.e., nearby low pressure center, high pressure center to the north, front) of increased water levels within the Delaware and Chesapeake Bays (Callahan et al. 2021). Of these, 106 TCs were identified as not being coincident to significant nontropical forcing on water levels. For each of the 106 TCs, a time window was determined encapsulating the TC's nearest approach to Delmarva and the maximum water level and surge observed at each tide gauge. For each extreme coastal flooding event defined in the previous section, the time of the maximum predicted tidal peak (for which skew surge was computed) was compared with all of the TC time windows. If the extreme coastal flooding event fell within a TC time window, it was designated as a TC event, else it was designated as a ML event. Note that all storm systems in IBTrACS are considered TCs for the current study, even if it transitioned to an ETC near the Delmarva Peninsula.

c. Comparison of skew surge and TWL between storm types

Extreme coastal flood events for TC and ML weather systems were compared in several ways. Mean surge and TWL were computed at each tide gauge and tested for differences using a two-sample *t* test. Variances of the distribution were also computed although were not quantitatively tested due to small sample size of TC events. The month of occurrence for each coastal flood event was extracted and seasonal distribution at each gauge was compared between weather system types.

The relative frequency of TCs (and therefore by contrast, of ML systems) was computed for sequential numbers of top events, in multiples of five up to 100, for both surge and TWL at each gauge. For example, using the ranked list of all surge events at the LEW gauge, the percentage of TCs occurring within the top five events was computed. This process was repeated for the top 10, top 15, ..., up to the top 100 events. Events ranked 80–100 generally had lower water levels than the 6-month RL, although this did not impact any results. Percentages were then averaged over all gauges within each of the four regions.

d. Top midlatitude skew surge events

Extreme surge events caused by ML weather systems were then investigated. Regional skew surge index values were computed by averaging the tide gauge SSIs over all gauges within each region for each ML extreme surge event, then ranked to generate a list of top ML surge events for each region. This is the same approach taken by Callahan et al. (2021) to generate a list of top TC regional surge events. A requirement for the current study is that the surge must have reached at least the 6-month RL at 2 of the 3 gauges within each region for it to be included as a regional extreme event. On only six occasions (4 at WAC, 1 at CAP, and 1 at ANN) data were not available at the third gauge, none of which were ranked in the top 10. Booth et al. (2016) also took a multisite approach when determining large surge events over an area from Massachusetts to Virginia. For the upper Delaware Bay region, surge must reach at least the 6month RL at either one of the two gauges.

Last, mean composites were generated of sea level pressure (SLP) and 500-hPa geopotential height (GPH) fields of the top 10 ML surge events. Modeled data were obtained from the National Centers for Environmental Prediction (NCEP) North American Regional Reanalysis (NARR) project, a long-term (1979-present), dynamically consistent, high-resolution, high-frequency, atmospheric and land surface hydrology dataset for the North American domain (Mesinger et al. 2006). Mean composites were produced from the 3-hourly, 0.3° gridded data product for 24 h prior (day -1) to 24 h after (day +1) the event, using the earliest time of maximum surge peak over all tide gauges within that region as the event time (day 0). Following Colle et al. (2010) and Catalano and Broccoli (2018), the 3-hourly modeled output (e.g., 0000, 0300, 0600, ..., 2100 UTC) just prior to the event time was used. For display purposes, contours were generated at 1-hPa and 25-m intervals for the SLP and 500-hPa GPH fields, respectively, after applying a 3 × 3 smoothing to the gridded data. Fields were compared between regions to associate the differences in synoptic meteorological conditions to differences in ML surge response.

The harmonic analysis was performed using the U-Tide package (Codiga 2011) in the Matlab programming environment. Other tidal data analyses and comparisons of weather

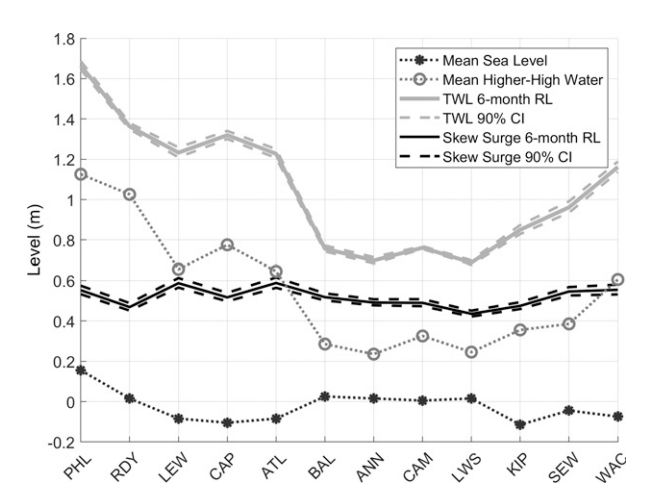


FIG. 2. Surge and total water level with 90% CIs for 6-month RL over 1980–2019. Mean higher-high water and mean sea level tidal data were published by NOAA over the 1983–2001 National Tidal Datum Epoch.

systems were also performed in Matlab. Temporal declustering was performed using the *POT* package (Ribatet and Dutang 2019) and the extreme value model fitting and RL extraction were performed using the *eva* package (Bader and Yan 2020) in the R statistical computing software environment. NARR model data were provided by the NOAA/OAR/ESRL/Physical Sciences Laboratory from their website (https://psl.noaa.gov/data/gridded/data.narr.html).

4. Results and discussion

a. Extreme value analysis of 6-month return levels

To compare extreme surges and TWL between weather systems, the 6-month RL was first extracted using POT/GP extreme value analysis after an appropriate threshold was selected, above which all of the exceedances were used to fit the GP distribution. Testing resulted in optimum threshold percentages of the surge distribution ranging from 93.5% at CAP to 99% at LEW, ANN, KIP, and SEW with no obvious spatial pattern. Testing on the TWL distribution resulted in optimum threshold percentages ranging from 95.5% to 97.0% at gauges within the lower bays and 97.5% to 99.5% in the upper bays.

TWL 6-month RLs in the Delaware Bay upper regions are larger than in its lower regions, whereas the reverse pattern holds for the Chesapeake Bay (Fig. 2). Overall largest values are found in the upper Delaware Bay (maximum of 1.66 m at PHL) and the smallest values in the central-to-upper Chesapeake Bay (minimums of 0.69 and 0.70 m at LWS and ANN, respectively.) Spatial pattern of the TWL 6-month RL matches that of the MHHW tidal datum as expected since areas with high MHHW also experience the largest tidal ranges and more easily reach the 6-month RL without the need for a major storm.

Surges (particularly measured as skew surges) in this region have much less spatial variation than tidally influenced TWL. The surge 6-month RLs range from 0.44 m at RDY to 0.59 m at LEW and ATL. Values in the central regions of each bay tend to be

smaller than the upper and lower regions. Largest values are found along the open ocean coast and on the southwest inside the lower bays. These locations are more directly impacted by onshore east-northeast winds from coastal storms, which build up water from local winds and increased volume of water into the bays form Ekman transport (due to southwest traveling ocean currents along the shoreline) and remote wind-driven surges.

Confidence intervals (CI) of the 6-month RLs are consistently narrow at all sites for both surge and TWL, driven by the large number of data points with small variance used to fit the GP model. For comparison and to test the POT/GP approach used in this paper, TWL RLs from 1- to 100-yr return periods were computed and compared with Nadal-Caraballo and Melby (2014). For the seven gauges analyzed in both studies, namely, LEW, CAP, ATL, BAL, ANN, CAM, and SEW, the 1-yr TWL RLs were 1.32, 1.46, 1.36, 0.89, 0.81, 0.84, and 1.13 m, respectively. These results differed from USACE (2014) by 0.02 m (LEW and CAM) to 0.06 m (BAL). Events with surge and TWL greater than the 6-month RL are defined as extreme for the remaining analysis in this paper.

b. Mean and distribution

Means of extreme surge are higher for TCs than for ML weather systems at all gauges (Table 2). Nine out of the 12 gauges (all except LEW, CAP, and WAC) show the difference to be statistically significant at the $\alpha = 0.05$ level. TC counts are relatively small, ranging from 8 at RDY and CAM to 20 at SEW, smaller by a factor of approximately 3-6 than ML weather system counts. Largest differences are generally in the upper bays, which support results in Callahan et al. (2021) showing most TCs stay to the south and east of Delmarva, causing larger surge response in the lower bays. The upper Chesapeake Bay shows the largest mean difference due to the particularly large surge generated by Hurricane Isabel and low number of TCs. For extreme TWL events, the patterns of smaller TC frequency and higher means are generally the same as it is for surge. Differences in the means are statistically significant at ATL in the Delaware Bay and at all sites (except WAC) in the Chesapeake Bay at the $\alpha = 0.05$ level.

Median values and overall distribution shapes are similar between weather systems for surge (Fig. 3, along with Fig. S2 in the online supplemental material) and TWL (Fig. S1 in the online supplemental material), resembling the extreme GP distribution, such as all of the data points greater than 1.5× interquartile range extend to the positive extreme rather than toward the lower end. Note that ML weather systems show more data points toward the positive extremes due to the larger number of ML events around the median decreasing the interquartile range. The absolute maximum and minimum of both surge and TWL are also similar between both weather types, aside from Hurricane Isabel in the upper Chesapeake. ML weather systems occur much more frequently but corresponding magnitudes and the distribution of flood levels are on par with TCs.

c. Month of occurrence

Seasonal distribution of extreme surge events has a well-defined temporal pattern (Fig. 4). Nearly all sites show

TABLE 2. Mean skew surge and total water level of extreme events caused by tropical cyclones and midlatitude weather systems over the period 1980–2019. Extreme events are defined as greater than the 6-month RL. The P values are the results of two-sample t tests; italicized results are statistically significant at the $\alpha = 0.05$ level.

	Total water level					Skew surge				
	Tropical		Midlatitude			Tropical		Midlatitude		
Station	Mean	N	Mean	N	P value	Mean	N	Mean	N	P value
Philadelphia	1.876	8	1.796	64	0.108	0.811	9	0.682	62	0.022
Reedy point	1.509	9	1.465	70	0.281	0.712	8	0.577	66	0.013
Lewes	1.460	11	1.392	63	0.232	0.791	14	0.765	64	0.614
Cape May	1.521	10	1.442	65	0.069	0.706	13	0.655	59	0.247
Atlantic City	1.499	8	1.345	72	0.004	0.894	9	0.728	75	0.004
Baltimore	1.039	11	0.848	71	0.001	0.852	9	0.645	65	0.006
Annapolis	0.925	13	0.785	67	0.004	0.721	11	0.597	68	0.025
Cambridge	0.946	12	0.840	68	0.002	0.726	8	0.586	69	0.002
Lewisetta	0.876	17	0.762	65	0.001	0.646	13	0.520	68	0.001
Kiptopeke	1.053	20	0.964	59	0.011	0.695	19	0.594	62	0.004
Sewells Point	1.206	23	1.110	60	0.040	0.818	20	0.707	60	0.025
Wachapreague	1.373	16	1.318	66	0.269	0.748	16	0.723	62	0.613

maximum ML surge event frequency in December or January with a significant number of events occurring throughout the cold season (October–April), except the lower Delaware Bay, which decreases in March. Very few ML or TC surge events occur during the summer (June–August). TC surge events are restricted to late summer through autumn (August–

November), with a maximum in September at all sites except for the lower Delaware Bay, with a maximum in October. Although many more ML than TC surge events occur over the course of a year, frequencies of extreme events caused by each weather type during the autumn season are similar. Early autumn (August–September) tends to have more TC

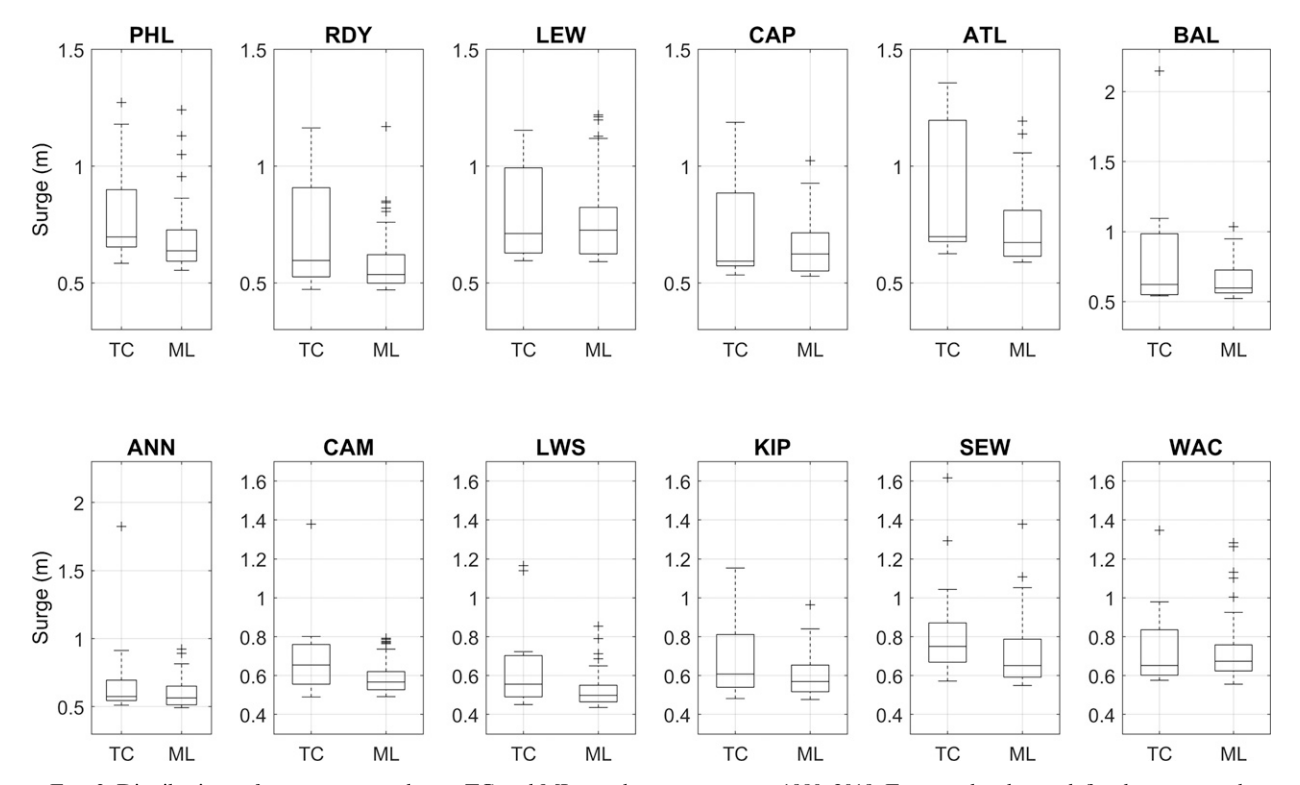


Fig. 3. Distributions of extreme surge due to TC and ML weather systems over 1980–2019. Extreme levels are defined as greater than the 6-month RL. Boxplots show medians, interquartile ranges (rectangular box), and $1.5\times$ interquartile range (hash marks). Data points (marked by plus signs) that are greater than the $1.5\times$ interquartile range are concentrated only toward the upper end of the distribution rather than the lower end.

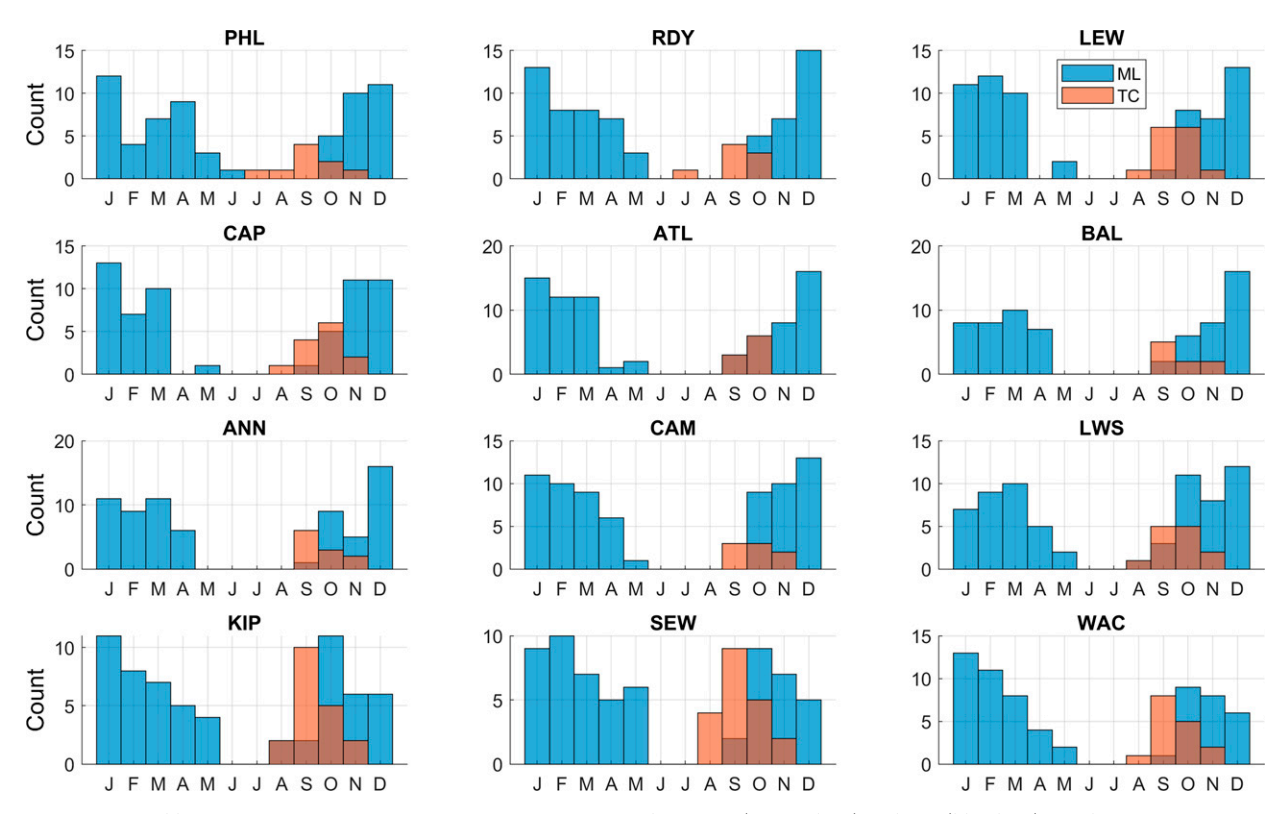


FIG. 4. Monthly frequency of occurrences of extreme surge events due to TC (orange bars) and ML (blue bars) weather systems over 1980–2019. Extreme levels are defined as greater than the 6-month RL.

events, whereas midautumn (October-November) tends to have more ML events.

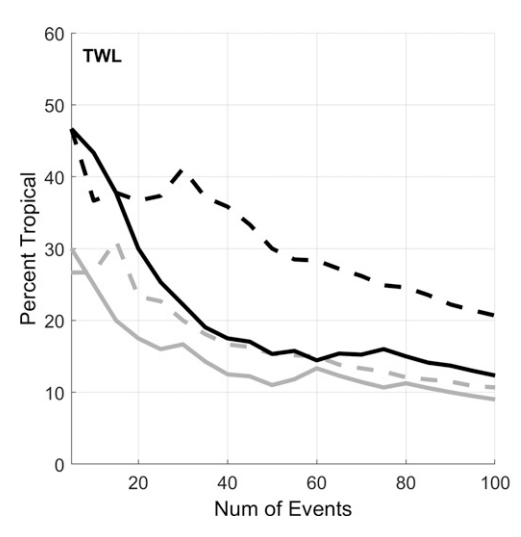
Seasonal distribution of extreme TWL events is similar to that of surge events but is more spread out over the year, demonstrating that coastal flooding is a threat to the mid-Atlantic during any month, except for July when very few events occur anywhere in the study area (Fig. S3 in the online supplemental material). ML TWL events in the upper Delaware Bay show noticeably low counts in February, lower than what seemingly can be attributed to its smaller number of days, and should be investigated further. All Chesapeake Bay sites show a maximum in October for ML TWL events. Upper and central regions have significantly fewer events during the winter months before a secondary peak in March. Combining both TC and ML TWL events for most sites show maximum occurrences in the early autumn and a secondary peak in the early spring, close to the seasonal distribution of MSL (NOAA CO-OPS 2020a). Seasonal peaks in MSL are due to 1) the high frequency of larger TC and ML storms and thermal expansion of coastal waters (early autumn peak), and 2) the high frequency of ML storms and large high tides while Earth is near the equinox yet not too far away from perihelion (early spring peak).

While the seasonal distribution of extreme TWL events is perhaps more closely related to mean sea levels, extreme surge is better characterized by storm intensity and tidal range. ML extreme surge events peak in the winter months when MSL is at a minimum and tidal ranges are large. This is

consistent with many previous studies (mentioned in the introduction) on the prevalence of wintertime ETCs, pressure gradients, and frontal systems. Tidal ranges in the summer months are minimal and MSLs are average (lower bays) to above average (upper bays). Lack of extreme surge events suggest the lack of strong coastal storms occurring during these months.

d. Relative frequency of weather systems

In all regions, the relative frequency of both extreme surge and TWL events from TCs decreases as the number of top events increases (Fig. 5). Of the top 20 TWL events, TCs cause approximately 35%-45% in the Chesapeake Bay and 20%-30% in the Delaware Bay. The lower Chesapeake Bay experiences the largest percent of TCs, 35%-45% in the top 10 events and 30% in the top 50 events, before declining alongside the other regions. For top surge events, the pattern is very similar, albeit with a few differences. The percent of TCs in the Delaware Bay is higher for the top 10 surge events (30%-45%) than for TWL but drops off more quickly. Upper Chesapeake Bay behaves nearly identically to the Delaware Bay regions whereas the lower Chesapeake Bay percent of TCs remains high, 40%-45% in the top 10 events and 25% in the top 50. These percentages asymptotically decrease to about 10%-15% (tested out to the top 200 events; not shown). From a ML perspective (Fig. S4 in the online supplemental material), the great majority of extreme surge events are from ML weather systems at 55%-70% in the top



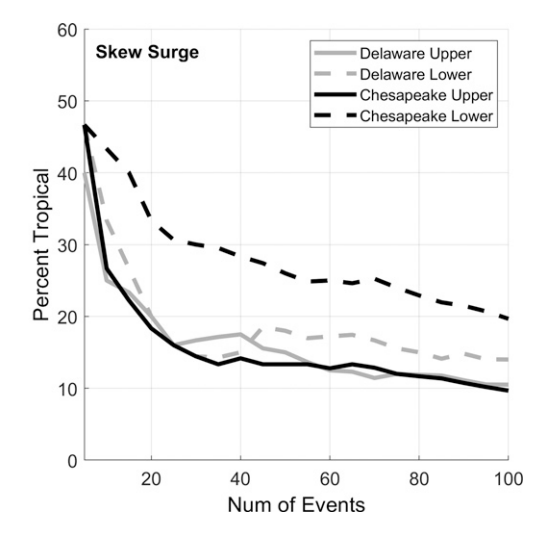


FIG. 5. Frequency of tropical cyclones of ranked total water level and surge events for regions within the Delaware (gray) and Chesapeake (black) Bays over 1980–2019. Solid lines represent the upper-bay regions, and dashed lines represent the lower-bay regions.

10 events and 80%–90% in the top 50 events for the Delaware Bay and upper Chesapeake Bay, and 55%–60% in the top 10 events and 75% in the top 50 events for the lower Chesapeake Bay. Using slightly different methods and sites farther south to Duck, North Carolina, Booth et al. (2016) found very similar results of TC percentages at 20%–60% for the top 10 events and 10%–30% for the top 50 events, with the larger values at the more southern locations.

TCs are known to impact U.S. Southeast coasts more often than mid-Atlantic and Northeast coasts, and Callahan et al. (2021) showed that most TCs that approached the Delmarva Peninsula stayed to the south and east directing winds and surge into the bays, so the result of the lower bays having a higher percentage of TC-caused large flood events was not entirely surprising. The upper and lower Delaware Bay showed similar behavior of TC percentages in both the TWL and surge cases, likely due to the bay smaller size and orientation to the coast, as compared with the much longer Chesapeake Bay where flood levels in the upper and lower regions have a more north-south and east-west dependence of the TC track. However, the quantification of the frequency of major coastal flooding events between TC and ML weather systems, particularly focused on the measure of skew surge, as well as demonstrating the differences between the upper and lower Chesapeake Bay regions, should prove useful for forecasting future risk for long-term planning and seasonal public awareness campaigns.

e. Top midlatitude skew surge events and synoptic composites

Table 3 shows the top 20 ML surge events for each region based on the mean storm surge index. The date/time is determined by the earliest tidal peak that reached the 6-month RL of all gauges within that region. Months of occurrence align well with Fig. 4, with the great majority of the top 20 events across all regions occurring in November–March and January

as the most common for the lower bays. Some overlap of ML events does occur among regions, most often between the lower (or upper) regions across the bays. Events on 4 January 1992, 5 February 1998, 25 January 2000, and 23 January 2016 are ranked in the top 10 for both lower Delaware and Chesapeake Bay regions. Likewise, the events on 12 February 1985, 28 November 1993, and 21 December 2012 are ranked in the top 10 for both upper-bay regions. However, no common events were ranked in the top 10 between the upper and lower Chesapeake Bay regions and only the 11 December 1992 event is common between the upper and lower Delaware Bay regions.

Mean synoptic conditions of the top 10 ML surge events were produced for each of the four regions to investigate the dominant weather conditions that result in extreme surges. In addition to the same geomorphologic and bathymetric factors that influence tides, surges along the coast are also influenced by coastal ocean currents, atmospheric surface pressure, wind speed and wind direction relative to the orientation of the coastline, and the size and speed of the weather system (Pore 1964; Pugh 2004; von Storch and Woth 2008; Ellis and Sherman 2015; Martzikos et al. 2021). The exact magnitudes of characteristics near the coast (where populated communities, and hence tide gauges, are located) are dependent upon the location and persistence of the large-scale synoptic patterns in place. Note that the current study focuses on coastal flooding events that produce the maximum peak meteorological contribution to surge, not the most damaging or most impactful storm events. Although maximum surges correlate well with wind strength and direction, several studies note the damage caused by coastal flooding is highly dependent upon the duration of an event (Dolan and Davis 1992; Grinsted et al. 2012; Bernhardt and DeGaetano 2012; Martzikos et al. 2021) and the relationship between maximum peak skew surge and duration in the mid-Atlantic is a timely topic for future research.

TABLE 3. Ranked regional surge events from midlatitude weather systems in the upper and lower Delaware and Chesapeake Bay regions over 1980–2019. Ranking is ordered by skew surge index, the mean of the normalized, detrended skew surges of all gauges within that region for that event. Date and time (UTC) represent the earliest tidal peak that reached the 6-month RL at gauges within a region.

	Upper Delaware		Lower Delaware		Upper Chesapea	Upper Chesapeake		Lower Chesapeake	
	Date	SSI	Date	SSI	Date	SSI	Date	SSI	
1	1054 21 Dec 2012	6.65	1030 29 Mar 1984	6.81	0236 5 Nov 1985	5.27	2318 12 Nov 2009	7.75	
2	1706 25 Oct 1980	5.42	0430 3 Mar 1994	6.70	0130 11 Mar 2011	4.87	0806 5 Feb 1998	7.07	
3	2242 2 Apr 2005	5.14	1242 4 Jan 1992	6.52	0030 5 Jan 1994	4.66	1654 25 Jan 2000	6.04	
4	2154 12 Feb 1985	4.69	0200 8 Jan 1996	6.34	0200 7 Mar 2018	4.58	1236 4 Jan 1992	5.92	
5	1500 28 Nov 1993	4.59	1242 23 Jan 2016	6.19	0748 21 Dec 2012	4.57	1542 19 Dec 2009	5.91	
6	0436 11 Dec 1992	4.57	0212 11 Dec 1992	6.19	0118 13 Feb 1985	4.57	0900 25 Oct 1982	5.78	
7	2230 4 Jan 1982	4.35	0806 5 Feb 1998	6.08	1200 28 Nov 1993	4.55	0254 2 Jan 1987	5.49	
8	1330 8 Nov 2012	4.32	2036 23 Jan 2017	6.02	1023 11 Dec 2003	4.49	1248 23 Jan 2016	5.36	
9	2012 14 Dec 2003	4.11	1554 25 Jan 2000	5.59	1724 25 Jan 2010	4.36	1542 10 Nov 1991	5.30	
10	1612 16 Apr 2018	4.06	1642 14 Nov 1995	5.48	1012 9 Feb 2016	4.12	1918 10 Apr 2003	5.27	
11	0242 17 Apr 2011	4.00	1418 25 Oct 1980	5.38	1630 17 Dec 2000	4.10	0806 6 Feb 2010	5.17	
12	0748 7 Mar 2018	3.85	1318 14 Mar 2017	5.36	2330 16 Nov 2006	4.03	2112 6 Mar 2013	5.06	
13	0424 9 Feb 2016	3.82	1612 7 Mar 2018	5.31	0612 4 Oct 2014	3.95	0554 4 Oct 2015	4.99	
14	0800 28 Oct 2006	3.81	1900 6 Mar 2013	5.26	2312 16 Apr 2011	3.93	0500 3 Mar 1994	4.91	
15	0648 5 Nov 1985	3.79	0612 4 Jan 1994	5.22	0830 11 Dec 1992	3.91	1748 22 Jan 1987	4.90	
16	2242 21 Mar 1980	3.78	1648 25 Dec 2002	5.11	2100 30 Sep 2010	3.90	1442 22 Nov 2006	4.87	
17	0036 3 Nov 1999	3.73	0718 21 Dec 2012	5.03	1200 28 Oct 2006	3.72	2254 23 Jan 2017	4.72	
18	0430 3 Dec 1986	3.71	1736 12 Feb 1985	4.97	1424 12 Feb 2015	3.72	1048 13 Apr 1988	4.71	
19	2206 10 Mar 2011	3.64	2312 11 Feb 1983	4.79	0224 25 Feb 2016	3.69	1336 28 Jan 1998	4.67	
20	0518 11 Dec 2003	3.56	0030 27 Dec 2012	4.73	0154 13 Dec 1983	3.69	1454 12 Dec 1992	4.64	

Figures 6 and 7 show the SLP and GPH mean composites, respectively, for the upper and lower Delaware Bay at 24 h prior (day -1), the same day (day 0), and 24 h after (day +1) the current event. A low pressure center (with cyclonic winds) is present to the west of Delmarva while a high pressure center (with anticyclonic winds) exists to the northeast in the days prior to the event. The presence of the semistationary high pressure to the north-northeast likely plays a large role in the buildup to peak flood levels as it results in tight pressure-gradient-driven easterly winds as the low continues to strengthen and progress toward Delmarva. For the top upperbay events, the low pressure center develops over the continental Midwest and travels east-northeast, usually directly over or staying to the northwest of Delmarva. Strong southeasterly winds blow up the bays increasing water levels before the low pressure center passes and winds reverse direction. For the top lower-bay events, the low pressure center develops in the southeast United States and travels northeast into coastal waters, staying offshore as it passes Delmarva. Since the low pressure centers for these lower-bay events occur more often over the warmer, less stable ocean surface than over land during the cold season (November-March), the pressure deepens further with stronger cyclonic winds than for the upper-bay events. The maximum difference of the low pressure centers between upper and lower bays events is approximately +11 hPa and located offshore to the southeast of Delmarva (Fig. S5 in the online supplemental material).

Mean composites of GPH for all regions show troughs in the Midwest on day 1, zonally propagating eastward. Areas of upper-level divergence, between the GPH trough and ridge, align with the surface low pressure centers to enhance cyclonic development near Delmarva. The GPH trough-ridge wave pattern is translated southward during top lower-bay events with maximum difference in heights of about 140 m (i.e., GPH for lower-bay events are 140 m shallower than for upper-bay events) located off the Southeast coast. Due to space limitations for this paper, mean composite maps for the Chesapeake Bay events are shown in Figs. S6–S8 in the online supplemental material. Similar spatial patterns to the Delaware Bay are exhibited for Chesapeake Bay events. The day 0 low pressure center for upper Chesapeake Bay events is elongated since some top upper Chesapeake Bay events stay farther west. Intensification of the low pressure center occurs slightly farther south for lower Chesapeake Bay events.

The GPH trough-ridge pattern and presence of the surface high pressure in the North Atlantic influences ETC storm tracks to travel in a more meridional northward pattern. Many studies have correlated the atmospheric blocking patterns in the North Atlantic in the cool season to more impactful and slower moving coastal storms along the U.S. mid-Atlantic and Northeast coasts (Colle et al. 2010; Bernhardt and DeGaetano 2012; Talke et al. 2014; Catalano and Broccoli 2018). Very similar SLP and GPH patterns were found in Leathers et al. (2011) who focused on meteorologically significant events to Delmarva by analyzing surface weather maps rather than tide gauge data. The combination of cyclonic low pressure centers intensifying over warmer waters under an area of upper-level divergence, traveling north-northeast along the coast due to the presence of anticyclonic high pressure center to the northeast makes for ripe conditions for strong, long-lasting storms in the mid-Atlantic. The setup is more prominent for the top 10 lower-bay events and resulted

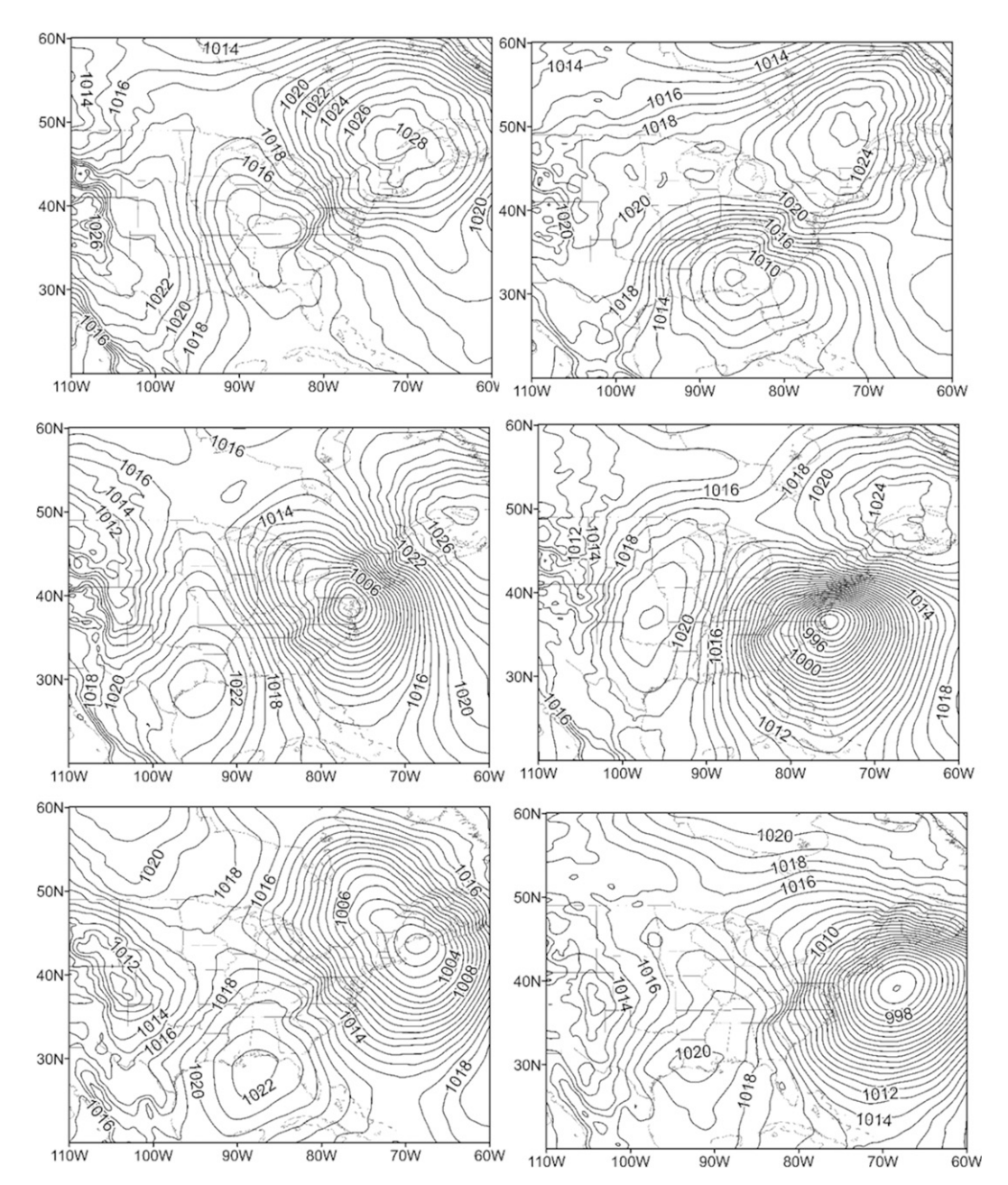


FIG. 6. Mean sea level pressure composite maps of the top 10 surge events in the (left) upper and (right) lower Delaware Bay caused by midlatitude weather systems, for (top) 24 h before the event, (middle) day of the event, and (bottom) 24 h after the event. Data are from the North American Regional Reanalysis project.

in higher SSI values for the lower regions (6.19 and 5.19) than for the upper regions (4.79 and 4.60) in the Delaware and Chesapeake Bays, respectively.

5. Conclusions

The scope of this study was to investigate the mean magnitude, distribution, time of year, and synoptic conditions (for ML events) of extreme coastal flooding events in the U.S. mid-Atlantic region over the past 40 years (1980–2019).

Analysis was performed on detrended TWL and surge values to account for SLR and other phenomena that would result in near-linear changes to water levels. This time period was the longest possible to adequately address the spatial variation within the Delaware and Chesapeake Bays based on tide gauge data availability. However, this study did not specifically address the temporal variations. Changes in the atmospheric circulation patterns (i.e., teleconnections) throughout the western Northern Hemisphere can alter storm tracks and ultimately coastal flood levels along the mid-Atlantic. Mean

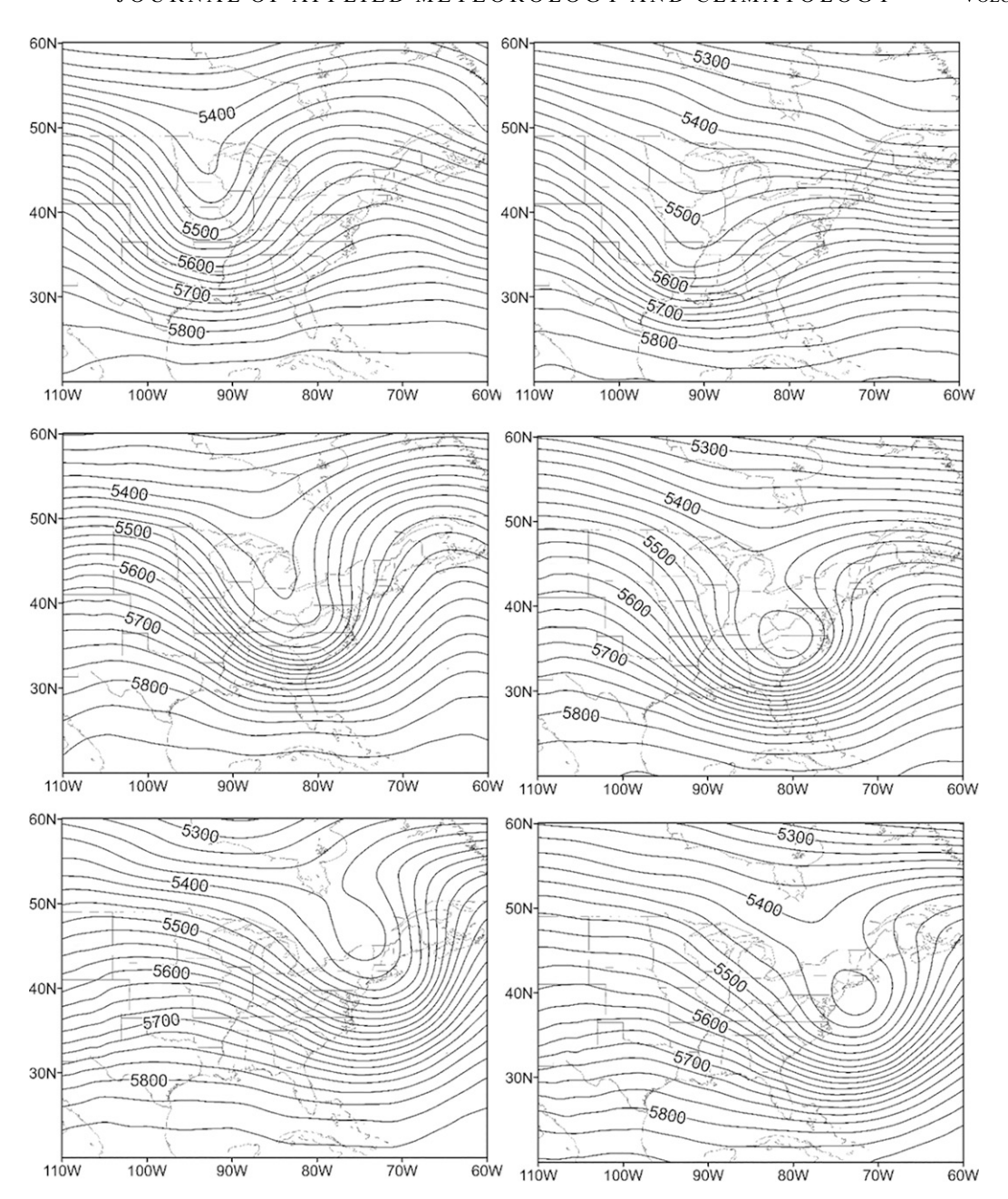


FIG. 7. As in Fig. 6, but for mean 500-hPa geopotential height.

SLP and GPH patterns found in this study are typical of the negative phase of the North Atlantic Oscillation (NAO), a measure of the difference in the semipermanent SLP regions of the Icelandic low and Azores high. Several studies have correlated the negative phase of the NAO, as well as the presence of El Niño or La Niña, to increased frequency of coastal storms and flood events (Sweet and Zervas 2011; Bernhardt and DeGaetano 2012; Thompson et al. 2013; Sweet et al. 2014; Talke et al. 2014; Sweet et al. 2020). Connections are more commonly found with increased frequency of coastal flooding rather than with the magnitude of surge levels. Some

studies have also found more complex relationships between coastal flood levels and multiple simultaneous atmospheric and oceanic oscillations (Ezer et al. 2013; Hamlington et al. 2015; Wahl and Chambers 2015; Catalano and Broccoli 2018; Kopp et al. 2019; Rashid et al. 2019; Little et al. 2019). Although the current study period was long enough to include multiple phases of many teleconnections, future research could focus on a few select gauges within the study area with much longer periods of record to better resolve temporal trend correlations, estimates of return levels, and identification of major coastal flooding events that took place before

1980, such as the Ash Wednesday Storm of 1962, still the storm of record for lower Delaware Bay coastal flood impacts.

This study assigned the "TC" designation to all cyclones in the IBTrACS database, even though some transitioned into ETCs or merged with frontal systems as they traveled through the mid-Atlantic region. It would be difficult to ascertain the exact time of extratropical transition, nonetheless, if these systems were designated as ML, the frequency of TCs in top events would likely decrease, and the prevailing synoptic patterns for SLP and GPH for top ML events may not have been as clear. Additional aspects of the current study may impact the robustness of the statistical results, although are likely minor. Selection of the 6-month RL was an arbitrary threshold for identifying extreme events. Although it yields enough data points to demonstrate patterns of surge yet represents flood levels at a magnitude that warrants preparation and planning, a lower or higher choice may have resulted in different statistics of the mean and distributions of extremes. A different approach to extreme value analysis modeling, such as using time-varying covariates, may have also resulted in a different 6-month return level. Likewise, the SLP and GPH mean composite maps may have been different if we had chosen a number greater or less than 10 or had used a fixed threshold value of SSI.

A few key messages were identified that will improve our understanding of the magnitude, spatial variation, and synoptic conditions conducive to extreme storm surges in the mid-Atlantic region.

- 1) Coastal flooding from TCs may get much of the attention, and justifiably have a higher mean surge level. ML weather systems can produce flood levels just as severe and occur much more frequently. Extreme ML events occur year-round (albeit rarely in June–August) while extreme TC events occur primarily in September–October. Over the course of the autumn season, counts of extreme TC and ML flood events are approximately equal, with typically more TC events in September and more ML events in October.
- 2) Within the Delaware Bay and upper Chesapeake Bay, TCs account for 30%–45% of top 10 and 15%–20% of the top 50 surge events. The lower Chesapeake Bay has a higher percentage of TC surge events at 40%–45% of the top 10 and 25% of the top 50. For both TWL and surge, the percent of TCs approaches 10%–15% for larger numbers of events.
- 3) Top ML surge events in the upper Delaware and Chesapeake Bays have strong similarities in synoptic conditions and top 10 lists. Lower regions across the bays also share these similarities, more so than with the opposing region in their own bay. This behavior was also found in Callahan et al. (2021) with regard to flood responses from TCs.
- 4) Mean SLP pattern for the top ML surge events consists of a low pressure center developing to the west of Delmarva (to the south for lower-bay events) and a semistationary high pressure center to the northeast. Strong pressuregradient easterly winds impacted the mid-Atlantic as the

- low travels east and intensifies. Low pressure centers were aligned with areas of upper-level divergence and the high pressure centers with GPH ridges. Low pressure centers during lower-bay events are located over warmer, unstable coastal waters and shifted southward relative to upper-bay events.
- 5) This study ranked the top surge events for the upper and lower regions of the Delaware and Chesapeake Bays from ML weather systems. Callahan et al. (2021) did the same for TCs using similar methods. Results from these two papers can be combined to form a list of top regional surge events for 1980–2019. Although NOAA also provides lists of top coastal flooding events over longer periods of time, those are based on observed TWL (not detrended surge) and only at individual tide gauges (not regions).

Acknowledgments. The authors thank NOAA for providing a large database of water-level data for public use and the NOAA Central Library Data Imaging Project for providing high-quality and easily accessible historical weather maps. Author Callahan also thanks Dr. Daniel L. Codiga, Graduate School of Oceanography, University of Rhode Island, and Dr. Richard Pawlowicz, Department of Earth, Ocean and Atmospheric Sciences, University of British Columbia, for their help in understanding the operation of U-Tide and performing harmonic analysis.

Data availability statement. The dataset of 6-month return level (with 90% confidence intervals) of TWLs and skew surges, as well as lists of top ML events for each subbay region of the Delaware and Chesapeake Bays, over the time period 1980–2019, can be found at the figshare repository (https://figshare.com/account/home#/projects/101741).

REFERENCES

Bader, B., and J. Yan, 2020: eva: Extreme value analysis with goodness-of-fit testing. R package, https://rdrr.io/cran/eva/.

Batstone, C., and Coauthors, 2013: A UK best-practice approach for extreme sea-level analysis along complex topographic coastlines. *Ocean Eng.*, 71, 28–39, https://doi.org/10.1016/j. oceaneng.2013.02.003.

Bernhardt, J. E., and A. T. DeGaetano, 2012: Meteorological factors affecting the speed of movement and related impacts of extratropical cyclones along the U.S. East Coast. *Nat. Hazards*, **61**, 1463–1472, https://doi.org/10.1007/s11069-011-0078-0.

Blake, E. S., and E. J. Gibney, 2011: The deadliest, costliest, and most intense United States tropical cyclones from 1851 to 2010 (and other frequently requested hurricane facts). NOAA Tech. Memo. NWS NHC-6, 49 pp., https://www.nhc. noaa.gov/pdf/nws-nhc-6.pdf.

Boesch, D. F., and Coauthors, 2018: Sea-level rise: Projections for Maryland 2018. University of Maryland Center for Environmental Science Rep., 27 pp., https://www.umces.edu/sites/ default/files/Sea-Level%20Rise%20Projections%20for%20 Maryland%202018_0.pdf.

- Boon, J. D., M. Mitchell, J. D. Loftis, and D. L. Malmquist, 2018: Anthropogenic sea level change: A history of recent trends observed in the U.S. East, Gulf and West Coast regions. Virginia Institute of Marine Science Special Rep. 467, 76 pp.
- Booth, J. F., H. E. Rider, and Y. Kushnir, 2016: Comparing hurricane and extratropical storm surge for the mid-Atlantic and northeast coast of the United States for 1979–2013. *Environ. Res. Lett.*, 11, 094004, https://doi.org/10.1088/1748-9326/11/9/094004.
- Callahan, J. A., and D. J. Leathers, 2021: Estimation of return levels for extreme skew surge coastal flooding events in the Delaware and Chesapeake Bays for 1980–2019. Front. Climate, 3, 684834, https://doi.org/10.3389/fclim.2021.684834.
- ——, B. P. Horton, D. L. Nikitina, C. K. Sommerfield, T. E. McKenna, and D. Swallow, 2017: Recommendation of sea-level rise planning scenarios for Delaware: Technical Report. Delaware Department of Natural Resources and Environmental Control, Delaware Coastal Programs Tech. Rep., 116 pp., https://southbethany.delaware.gov/files/2018/11/ Attachment-6-to-February-2018-Mayor-Report-Technical-Report-Regarding-SLR-Planning-Scenarios.pdf.
- —, D. J. Leathers, and C. L. Callahan, 2021: Skew surge and storm tides of tropical storms in the Delaware and Chesapeake Bays for 1980–2019. Front. Climate, 3, 610062, https:// doi.org/10.3389/fclim.2021.610062.
- Catalano, A. J., and A. J. Broccoli, 2018: Synoptic characteristics of surge-producing extratropical cyclones along the northeast coast of the United States. J. Appl. Meteor. Climatol., 57, 171–184, https://doi.org/10.1175/JAMC-D-17-0123.1.
- Chesapeake Bay Program, 2020: State of the Chesapeake.

 Accessed 18 August 2020, https://www.chesapeakebay.net/
- Codiga, D. L., 2011: Unified tidal analysis and prediction using the UTide Matlab functions. University of Rhode Island Graduate School of Oceanography Tech. Rep. 2011-01, 60 pp.
- Colle, B. A., K. Rojowsky, and F. Buonaito, 2010: New York City storm surges: Climatology and an analysis of the wind and cyclone evolution. *J. Appl. Meteor. Climatol.*, 49, 85–100, https://doi.org/10.1175/2009JAMC2189.1.
- —, J. F. Booth, and E. K. M. Chang, 2015: A review of historical and future changes of extratropical cyclones and associated impacts along the US East Coast. *Curr. Climate Change Rep.*, 1, 125–143, https://doi.org/10.1007/s40641-015-0013-7.
- Council on Climate Preparedness and Resilience, 2016: Opportunities to enhance the nation's resilience to climate change. U.S. government Rep., 46 pp., https://obamawhitehouse.archives.gov/sites/default/files/finalresilienceopportunitiesreport.pdf.
- Dahl, K. A., M. F. Fitzpatrick, and E. Spanger-Siegfried, 2017: Sea level rise drives increased tidal flooding frequency at tide gauges along the U.S. East and Gulf Coasts: Projections for 2030 and 2045. PLOS ONE, 12, e0170949, https://doi.org/10. 1371/journal.pone.0170949.
- DeGaetano, A. T., 2008: Predictability of seasonal east coast winter storm surge impacts with application to New York's Long Island. *Meteor. Appl.*, 15, 231–242, https://doi.org/10. 1002/met.59.
- Delaware Emergency Management Agency, 2018: State of Delaware all-hazard mitigation plan. DEMA Doc., 308 pp., https://dema.delaware.gov/contentFolder/pdfs/HazardMitigationPlan.pdf.
- Dolan, R., and R. Davis, 1992: An intensity scale for Atlantic coast northeast storms. J. Coastal Res., 8, 840–853.

- Domingues, R., and Coauthors, 2020: Sea level hot spots from Florida to Maine: Drivers, impacts, and adaptation. U.S. CLI-VAR Rep. 2020-2, 40 pp., https://doi.org/10.5065/nk2v-pw16.
- Dupigny-Giroux, L. A., and Coauthors, 2018: Northeast. *Impacts, Risks, and Adaptation in the United States: Fourth National Climate Assessment*, D. R. Reidmiller et al., Eds., Vol. II, U.S. Global Change Research Program, 669–742, https://doi.org/10.7930/NCA4.2018.CH18.
- Ellis, J. T., and D. J. Sherman, 2015: Perspectives on coastal and marine hazards and disasters. *Coastal Marine Hazards, Risks, and Disasters*, J. F. Shroder, J. T. Ellis, and D. J. Sherman, Eds., Hazards and Disasters Series, Elsevier, 1–13, https://doi.org/10.1016/B978-0-12-396483-0.01001-3.
- Ezer, T., L. P. Atkinson, W. B. Corlett, and J. L. Blanco, 2013: Gulf Stream's induced sea level rise and variability along the U.S. mid-Atlantic coast. *J. Geophys. Res. Oceans*, 118, 685–697, https://doi.org/10.1002/jgrc.20091.
- Garner, A. J., and Coauthors, 2017: Impact of climate change on New York City's coastal flood hazard: Increasing flood heights from the preindustrial to 2300 CE. *Proc. Natl. Acad. Sci. USA*, **114**, 11861–11866, https://doi.org/10.1073/pnas. 1703568114
- Grinsted, A., J. C. Moore, and S. Jevrejeva, 2012: Homogeneous record of Atlantic hurricane surge threat since 1923. *Proc. Natl. Acad. Sci. USA*, 109, 19601, https://doi.org/10.1073/pnas. 1209542109.
- Haaf, L., S. Demberger, D. Kreeger, and E. Baumbach, Eds., 2017: Technical report for the Delaware Estuary and Basin 2017. Partnership for the Delaware Estuary Rep. 17-07, 379 pp., https://s3.amazonaws.com/delawareestuary/TREB+ douments/TREB+2017+complete.pdf.
- Hall, J. A., S. Gill, J. Obeysekera, W. Sweet, K. Knuuti, and J. Marburger, 2016: Regional Sea Level Scenarios for Coastal Risk Management: Managing the Uncertainty of Future Sea Level Change and Extreme Water Levels for Department of Defense Coastal Sites Worldwide. U.S. Department of Defense Strategic Environmental Research and Development Program, 224 pp.
- Hallegatte, S., C. Green, R. J. Nicholls, and J. Corfee-Morlot, 2013: Future flood losses in major coastal cities. *Nat. Climate Change*, 3, 802–806, https://doi.org/10.1038/nclimate1979.
- Hamlington, B. D., R. R. Leben, K.-Y. Kim, R. S. Nerem, L. P. Atkinson, and P. R. Thompson, 2015: The effect of the El Niño-Southern Oscillation on U.S. regional and coastal sea level. *J. Geophys. Res. Oceans*, 120, 3970–3986, https://doi.org/10.1002/2014JC010602.
- Harris, D. L., 1991: Reproducibility of the harmonic constants. *Tidal Hydrodynamics*, B. P. Parker, Ed., John Wiley and Sons, 753–771.
- Hinkel, J., and Coauthors, 2014: Coastal flood damage and adaptation costs under 21st century sea-level rise. *Proc. Natl. Acad. Sci. USA*, **111**, 3292–3297, https://doi.org/10.1073/pnas. 1222469111.
- Hirsch, M. E., A. T. Degaetano, and S. J. Colucci, 2001: An East Coast winter storm climatology. *J. Climate*, **14**, 882–899, https://doi.org/10.1175/1520-0442(2001)014<0882:AECWSC>2. 0.CO;2.
- Holgate, S. J., and Coauthors, 2013: New data systems and products at the permanent service for mean sea level. *J. Coastal Res.*, 29, 493–504, https://doi.org/10.2112/JCOASTRES-D-12-00175.1.
- Knapp, K. R., H. J. Diamond, J. P. Kossin, M. C. Kruk, and C. J. Schreck, 2018: International Best Track Archive for

- Climate Stewardship (IBTrACS) Project, Version 4. Subset used: North Atlantic Basin since 1980, NOAA/National Centers for Environmental Information, accessed 18 May 2020, https://doi.org/10.25921/82ty-9e16.
- Knutson, T., and Coauthors, 2019: Tropical cyclones and climate change assessment: Part I: Detection and attribution. *Bull. Amer. Meteor. Soc.*, **100**, 1987–2007, https://doi.org/10.1175/BAMS-D-18-0189.1.
- —, and Coauthors, 2020: Tropical cyclones and climate change assessment: Part II: Projected response to anthropogenic warming. *Bull. Amer. Meteor. Soc.*, **101**, E303–E322, https:// doi.org/10.1175/BAMS-D-18-0194.1.
- Kopp, R. E., K. Hayhoe, D. R. Easterling, T. Hall, R. Horton, K. E. Kunkel, and A. N. LeGrande, 2017: Potential surprises—Compound extremes and tipping elements. *Climate Science Special Report: Fourth National Climate Assessment*, D. J. Wuebbles et al., Eds., Vol. I, U.S. Global Change Research Program, 411–429, https://doi.org/10.7930/J0GB227J.
- —, E. A. Gilmore, C. M. Little, J. Lorenzo-Trueba, V. C. Ramenzoni, and W. V. Sweet, 2019: Usable science for managing the risks of sea-level rise. *Earth's Future*, 7, 1235–1269, https://doi.org/10.1029/2018EF001145.
- Leathers, D. J., R. Scarborough, and D. R. Legates, 2011: Delaware coastal storm climatology and damage assessment, 1871–2009: Final report. Delaware Department of Natural Resources and Environmental Control Rep., 20 pp.
- Lee, S. B., M. Li, and F. Zhang, 2017: Impact of sea level rise on tidal range in Chesapeake and Delaware Bays. J. Geophys. Res. Oceans, 122, 3917–3938, https://doi.org/10.1002/ 2016JC012597.
- Lin, N., K. Emanuel, M. Oppenheimer, and E. Vanmarcke, 2012: Physically based assessment of hurricane surge threat under climate change. *Nat. Climate Change*, 2, 462–467, https://doi. org/10.1038/nclimate1389.
- —, R. E. Kopp, B. P. Horton, and J. P. Donnelly, 2016: Hurricane Sandy's flood frequency increasing from 1800 to 2100. Proc. Natl. Acad. Sci. USA, 113, 12071–12075, https://doi.org/10.1073/pnas.1604386113.
- —, R. Marsooli, and B. A. Colle, 2019: Storm surge return levels induced by mid-to-late-twenty-first-century extratropical cyclones in the northeastern United States. *Climatic Change*, 154, 143–158, https://doi.org/10.1007/s10584-019-02431-8.
- Little, C. M., A. Hu, C. W. Hughes, G. D. McCarthy, C. G. Piecuch, R. M. Ponte, and M. D. Thomas, 2019: The relationship between U.S. East Coast sea level and the Atlantic meridional overturning circulation: A review. *J. Geophys. Res. Oceans*, 124, 6435, https://doi.org/10.1029/2019JC015152.
- Martzikos, N. T., P. E. Prinos, C. D. Memos, and V. K. Tsoukala, 2021: Key research issues of coastal storm analysis. *Ocean Coastal Manage.*, 199, 105389, https://doi.org/10.1016/j.ocecoaman. 2020.105389.
- Mawdsley, R. J., and J. D. Haigh, 2016: Spatial and temporal variability and long-term trends in skew surges globally. Front. Mar. Sci., 3, 1–29, https://doi.org/10.3389/fmars.2016.00029.
- Merrifield, M. A., A. S. Genz, C. P. Kontoes, and J. J. Marra, 2013: Annual maximum water levels from tide gauges: Contributing factors and geographic patterns. *J. Geophys. Res. Oceans*, 118, 2535–2546, https://doi.org/10.1002/jgrc.20173.
- Mesinger, F., and Coauthors, 2006: North American Regional Reanalysis. Bull. Amer. Meteor. Soc., 87, 343–360, https://doi. org/10.1175/BAMS-87-3-343.
- Michaelis, A. C., J. Willison, G. M. Lackmann, and W. A. Robinson, 2017: Changes in winter North Atlantic extratropical

- cyclones in high resolution regional pseudo–global warming simulations. *J. Climate*, **30**, 6905–6925, https://doi.org/10.1175/JCLI-D-16-0697.1.
- Moftakhari, H. R., A. AghaKouchak, B. F. Sanders, D. L. Feldman, W. V. Sweet, R. A. Matthew, and A. Luke, 2015: Increased nuisance flooding along the coasts of the United States due to sea level rise: Past and future. *Geophys. Res. Lett.*, 42, 9846–9852, https://doi.org/10.1002/2015GL066072.
- Muis, S., M. I. Apecechea, J. Dullaart, J. de Lima Rego, K. S. Madsen, J. Su, K. Yan, and M. Verlaan, 2020: A high-resolution global dataset of extreme sea levels, tides, and storm surges, including future projections. *Front. Mar. Sci.*, 7, 263, https://doi.org/10.3389/fmars.2020.00263.
- Nadal-Caraballo, N. C., and J. A. Melby, 2014: North Atlantic Coast Comprehensive Study Phase I: Statistical analysis of historical extreme water levels with sea level change. U.S. Army Engineer Research and Development Center Coastal and Hydraulics Laboratory Tech. Rep. ERDC/CHL TR-14-7, 125 pp., https://usace.contentdm.oclc.org/digital/collection/p26 6001coll1/id/3665/.
- NOAA, 2020a: PORTS (Physical Oceanographic Real-Time System). NOAA Tides and Currents, accessed 18 August 2020, https://tidesandcurrents.noaa.gov/ports.html.
- ——, 2020b: National Ocean Service National Water Level Observation Network (NWLON). NOAA Tides and Currents, accessed 18 August 2020, https://www.tidesandcurrents. noaa.gov/nwlon.html.
- NOAA CO-OPS, 2020a: Sea level trends. NOAA Tides and Currents, accessed 18 August 2020, https://tidesandcurrents.noaa.gov/sltrends/.
- —, 2020b: API for data retrieval. NOAA Tides and Currents, accessed 9 April 2020, https://api.tidesandcurrents.noaa.gov/ api/prod/.
- ——, 2020c: NOAA tide predictions. NOAA Tides and Currents, accessed 9 April 2020, https://tidesandcurrents.noaa.gov/tide_ predictions.html.
- Oppenheimer, M., and Coauthors, 2019: Sea level rise and implications for low-lying islands, coasts and communities. *The Ocean and Cryosphere in a Changing Climate*, H.-O. Pörtner et al., Eds., IPCC, 321–445.
- Orton, P. M., T. M. Hall, S. A. Talke, A. F. Blumberg, N. Georgas, and S. Vinogradov, 2016: A validated tropical-extratropical flood hazard assessment for New York Harbor. *J. Geophys. Res. Oceans*, 121, 8904–8929, https://doi.org/10.1002/2016JC011679.
- Parker, B. B., 2007: Tidal analysis and prediction. NOAA Special Publ. NOS CO-OPS 3, 388 pp., https://tidesandcurrents.noaa. gov/publications/Tidal_Analysis_and_Predictions.pdf.
- Piecuch, C. G., P. Huybers, C. C. Hay, A. C. Kemp, C. M. Little, J. X. Mitrovica, R. M. Ponte, and M. P. Tingley, 2018: Origin of spatial variation in US East Coast sea-level trends during 1900–2017. *Nature*, 564, 400–404, https://doi.org/10.1038/ s41586-018-0787-6.
- Pore, N. A., 1964: The relation of wind and pressure to extratropical storm surge at Atlantic City. *J. Appl. Meteor.*, **3**, 155–163, https://doi.org/10.1175/1520-0450(1964)003<0155:TROWAP>2.
- Pugh, D., 2004: Changing Sea Levels: Effects of Tides, Weather, and Climate. Cambridge University Press, 265 pp.
- —, and P. Woodworth, 2014: Sea-Level Science: Understanding Tides, Surges, Tsunamis and Mean Sea-Level Changes. Cambridge University Press, 395 pp.

- Rahmstorf, S., 2017: Rising hazard of storm-surge flooding. *Proc. Natl. Acad. Sci. USA*, **114**, 11806–11808, https://doi.org/10.1073/pnas.1715895114.
- Rajan, C. M., and S. J. Saud, 2018: Storm surge and its effect—A review on disaster management in coastal areas. *Civil Eng. Res. J.*, **4**, 555649, https://doi.org/10.19080/CERJ.2018.04. 555649.
- Ramsey, K. W., D. J. Leathers, D. V. Wells, and J. H. Talley, 1998: Summary Report: The coastal storms of January 27–29 and February 4–6, 1998, Delaware and Maryland. Delaware Geological Survey Open File Rep. 40, 47 pp., https://www.dgs.udel.edu/sites/default/files/publications/OFR40.pdf.
- Rappaport, E., 2014: Fatalities in the United States from Atlantic tropical cyclones new data and interpretation. *Bull. Amer. Meteor. Soc.*, 95, 341–346, https://doi.org/10.1175/BAMS-D-12-00074.1.
- Rashid, M., T. Wahl, D. Chambers, F. Calafat, and W. Sweet, 2019: An extreme sea level indicator for the contiguous United States coastline. Sci. Data, 6, 326, https://doi.org/10. 1038/s41597-019-0333-x.
- Ribatet, M., and C. Dutang, 2019: POT: Generalized Pareto distribution and peaks over threshold. R package version 1.1-7, https://cran.r-project.org/web/packages/POT/index.html.
- Ross, A. C., R. G. Najjar, M. Li, S. B. Lee, F. Zhang, and W. Liu, 2017: Fingerprints of sea level rise on changing tides in the Chesapeake and Delaware Bays. *J. Geophys. Res. Oceans*, 122, 8102–8125, https://doi.org/10.1002/2017JC012887.
- Sallenger, A. H., K. S. Doran, and P. A. Howd, 2012: Hotspot of accelerated sea-level rise on the Atlantic coast of North America. *Nat. Climate Change*, 2, 884–888, https://doi.org/10. 1038/nclimate1597.
- Salmun, H., A. Molod, K. Wisniewska, and F. S. Buonaiuto, 2011: Statistical prediction of the storm surge associated with coolweather storms at the Battery, New York. J. Appl. Meteor. Climatol., 50, 273–282, https://doi.org/10.1175/2010JAMC2459.1.
- Sanchez, J. R., G. Kauffman, K. Reavy, and A. Homsey, 2012: Natural capital value. Technical report for the Delaware Estuary and Basin 2017, Partnership for the Delaware Estuary Rep. 17-07, 70-75.
- Stephens, S. A., R. G. Bell, and I. D. Haigh, 2020: Spatial and temporal analysis of extreme storm-tide and skew-surge events around the coastline of New Zealand. *Nat. Hazards Earth Syst. Sci.*, 20, 783–796, https://doi.org/10.5194/nhess-20-783-2020.
- Sweet, W. V., and C. Zervas, 2011: Cool-season sea level anomalies and storm surges along the U.S. East Coast: Climatology and comparison with the 2009/10 El Nino. *Mon. Wea. Rev.*, 139, 2290–2299, https://doi.org/10.1175/MWR-D-10-05043.1.
- —, J. Park, J. J. Marra, C. E. Zervas, and S. Gill, 2014: Sea level rise and nuisance flood frequency changes around the United States. NOAA Tech. Rep. NOS CO-OPS 073, 66 pp., https://tidesandcurrents.noaa.gov/publications/NOAA_Technical_Report_NOS_COOPS_073.pdf.
- —, —, S. Gill, and J. Marra, 2015: New ways to measure waves and their effects at NOAA tide gauges: A Hawaiian-network perspective. *Geophys. Res. Lett.*, 42, 9355–9361, https://doi.org/10.1002/2015GL066030.
- —, R. M. Horton, R. E. Kopp, A. N. LeGrande, and A. Romanou, 2017a: Sea level rise. Climate Science Special Report: Fourth National Climate Assessment, D. J. Wuebbles et al.,

- Eds., Vol. I, U.S. Global Change Research Program, 333–363, https://doi.org/10.7930/J0VM49F2.
- —, R. E. Kopp, C. P. Weaver, J. Obeysekera, R. M. Horton, E. R. Thieler, and C. Zervas, 2017b: Global and regional sea level rise scenarios for the United States. NOAA Tech. Rep. NOS CO-OPS 083, 75 pp., https://tidesandcurrents.noaa.gov/ publications/techrpt83_Global_and_Regional_SLR_Scenarios_ for_the_US_final.pdf.
- —, G. Dusek, J. Obeysekera, and J. J. Marra, 2018: Patterns and projections of high tide flooding along the U.S. coastline using a common impact threshold. NOAA Tech. Rep. NOS CO-OPS 086, 56 pp., https://tidesandcurrents.noaa.gov/publications/techrpt86_PaP_of_HTFlooding.pdf.
- Sweet, W., G. Dusek, G. Carbin, J. Marra, D. Marcy, and S. Simon, 2020: 2019 state of U.S. high tide flooding with a 2020 outlook. NOAA Tech. Rep. NOS CO-OPS 092, 24 pp., https://tidesandcurrents.noaa.gov/publications/Techrpt_092_ 2019_State_of_US_High_Tide_Flooding_with_a_2020_Outlook_ 30June2020.pdf.
- Taherkhani, M., S. Vitousek, P. Barnard, N. Frazer, T. Anderson, and C. Fletcher, 2020: Sea-level rise exponentially increases coastal flood frequency. Sci. Rep., 10, 6466, https://doi.org/10.1038/s41598-020-62188-4.
- Talke, S. A., P. Orton, and D. A. Ray, 2014: Increasing storm tides in New York Harbor, 1844–2013. *Geophys. Res. Lett.*, 41, 3149–3155, https://doi.org/10.1002/2014GL059574.
- Thompson, P. R., G. T. Mitchum, C. Vonesch, and J. Li, 2013: Variability of winter storminess in the eastern United States during the twentieth century from tide gauges. *J. Climate*, 26, 9713–9726, https://doi.org/10.1175/JCLI-D-12-00561.1.
- von Storch, H., and K. Woth, 2008: Storm surges, perspectives, and options. Sustain. Sci., 3, 33–43, https://doi.org/10.1007/ s11625-008-0044-2.
- Wahl, T. V., and D. P. Chambers, 2015: Evidence for multidecadal variability in US extreme sea level records. J. Geophys. Res. Oceans, 120, 1527–1544, https://doi.org/10.1002/2014JC010443.
- Weinkle, J., C. Landsea, D. Collins, R. Musulin, R. P. Crompton, P. K. Klotzbach, and R. Pielke Jr., 2018: Normalized hurricane damage in the continental United States 1900–2017. Nat. Sustain., 1, 808–813, https://doi.org/10.1038/s41893-018-0165-2.
- Wilkerson, C. N., and J. Brubaker, 2012: Analysis of extreme water levels in the lower Chesapeake Bay. *Proc. 2012* OCEANS Conf., Hampton Roads, VA, Institute of Electrical and Electronics Engineers, https://doi.org/10.1109/OCEANS. 2012.6405098.
- Williams, J., K. J. Horsburgh, J. A. Williams, and R. N. F. Proctor, 2016: Tide and skew surge independence: New insights for flood risk. *Geophys. Res. Lett.*, 43, 6410–6417, https://doi.org/ 10.1002/2016GL069522.
- Wong, K.-C., and A. Münchow, 1995: Buoyancy forced interaction between estuary and inner shelf: Observation. Cont. Shelf Res., 15, 59–88, https://doi.org/10.1016/0278-4343(94) P1813-Q.
- Zhang, K., B. C. Douglas, and S. P. Leatherman, 2000: Twentieth-century storm activity along the U.S. East Coast. *J. Climate*, **13**, 1748–1761, https://doi.org/10.1175/1520-0442(2000)013 <1748:TCSAAT>2.0.CO;2.
- Zhong, L., and M. Li, 2006: Tidal energy fluxes and dissipation in the Chesapeake Bay. *Cont. Shelf Res.*, **26**, 752–770, https://doi.org/10.1016/j.csr.2006.02.006.